

Corrosion Inhibition of Mg-Al-Zn Alloy in Neutral Chloride Solutions by N-Acetyl-Cysteine as Eco-Friendly Material

W. A. Badawy, H. Nady and G. M. Abd El-Hafez

Chemistry Department, Faculty of Science, Cairo University, 12 613 Giza- Egypt

Chemistry Department, Faculty of Science, Fayoum University, Fayoum-Egypt

Abstract - The electrochemical behavior of Mg-7%Al-1%Zn alloy was investigated in neutral chloride solutions. Potentiodynamic experiments and electrochemical impedance spectroscopy were used. The increase of chloride ion concentration leads to an increase in the corrosion rate of the alloy. The electrochemical measurements were complemented by scanning electron microscopy and EDAX investigations. The results show that N-acetyl-cysteine is an effective corrosion inhibitor for the Mg-alloy corrosion in neutral chloride solutions at very low concentrations. The corrosion inhibition efficiency is >95% at 10 mM N-acetyl-cysteine. The process is based on adsorption of the molecules on the alloy surface and its mechanism was discussed.

Keywords: Corrosion inhibition, EIS, Magnesium alloy, N-acetyl-cysteine.

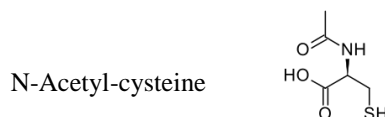
I. INTRODUCTION

In the last decades, the importance of magnesium alloys was increased significantly in various industries due to the high strength/weight ratio, high dimensional stability, good machining, and recyclability [1]. The poor corrosion resistance is one of the major problems that prevent the widespread of magnesium alloys in outdoor applications due to high chemical and electrochemical activity compared with other structural materials such as steels and Al alloys. There are two primary reasons for the poor corrosion resistance of magnesium alloys; the first is the internal galvanic corrosion due to second phases or impurities; and the second reason is that the barrier film formed on magnesium is much less stable than the passive films formed on other materials [2]. The electrochemical behavior of magnesium alloy in different solutions has attracted many research groups [3]–[9]. It was agreed that the solution pH has a dominant effect on the corrosion resistance of these alloys [10]–[11]. The alloying elements, precipitations, microstructure, and grain size are the main precursor of corrosion processes in the magnesium alloys in neutral chloride solutions [2,3,10]. Alloys containing low amounts of iron, copper and nickel were found to be more corrosion resistant. Surface pretreatment is essential for protection against corrosion and is usually required if aggressive electrolytes are used [3,10]. Some surface pretreatments such as chromate/manganese treatment were employed in order to improve the corrosion resistance of magnesium alloys in commercial applications [12]. Chromate containing materials are extremely hazardous and their

use and disposal are highly restricted worldwide [12]. It is necessary to explore other eco-friendly materials that can be used for pretreatments or as corrosion inhibitors to provide suitable and durable protection for magnesium alloys. Natural products of plant origins as well as some nontoxic organic compounds, which contain functional groups containing nitrogen, oxygen, and/or sulfur or even conjugated systems in their molecules, show promising results as corrosion inhibitors [13]–[21]. The mechanism of the corrosion inhibition process is usually attributed to adsorption of these molecules on the active centers of the metallic surface preventing its direct interaction with the corrosive medium. In this paper we are using an eco-friendly amino acid derivative, namely N-acetyl-cysteine as inhibitor for the corrosion of Mg-Al-Zn in stagnant naturally aerated neutral NaCl solutions. The corrosion rate and corrosion inhibition efficiency were calculated at different concentrations of the inhibitor. In this respect, conventional electrochemical techniques such as potential dynamic polarization and electrochemical impedance spectroscopy, EIS, were used. The experimental impedance data were fitted to theoretical values according to equivalent circuit models, which enable understanding the corrosion inhibition mechanism and the suggestion of the suitable model that explains the electrochemical behavior of the metal/solution interface under different conditions. The surface morphology of the alloy after immersion in NaCl solution was examined by SEM and the constituents of the alloy surface were analyzed by EDAX.

II. METHODOLOGY

The inhibitor used in these investigations was purchased from Sigma–Aldrich and have the following structure.



As can be seen, each molecule has three active groups, which can act as adsorption centers. The working electrodes were made as massive rods from commercial grade Mg–Al–Zn alloy of the composition 92, 7 and 1 for Mg, Al and Zn in mass%, respectively. The electrodes were mounted into glass tubes by two-component epoxy resin leaving a surface area of 0.2 cm² to contact the corrosive medium. The electrochemical cell was a three-electrode all-glass cell, with a large area platinum counter

electrode and a saturated calomel reference electrode. Before each experiment, the working electrode was abraded using successive grades emery papers down to 2000 grit, rubbed with a smooth polishing cloth, then washed thoroughly with triple distilled water and transferred quickly to the electrochemical cell. The measurements were carried out in aqueous solutions, where analytical grade reagents and triply distilled water were always used. The test solution was a stagnant naturally aerated aqueous buffer solution of pH 7, prepared by mixing 113.6mL 0.1M KH₂PO₄ + 56.8mL 0.1MNaOH+ 79.6mL H₂O. The effect of chloride ion concentration was studied by the addition of various amounts of NaCl ranging from 0.1 to 0.4M. The corrosion inhibition investigations were carried out in stagnant naturally aerated neutral 0.2 M Cl⁻ by different concentrations of N-acetyl-cysteine. The polarization experiments and electrochemical impedance spectroscopic investigations, EIS, were performed using a VoltalabPGZ 100 “All-in-one” potentiostat/Galvanostat system. The potentials were measured against and referred to the saturated calomel electrode, SCE (0.245 V vs the standard hydrogen electrode, SHE). All potential dynamic polarization experiments were carried out using a scan rate of 10 mV s⁻¹. The impedance, Z, and phase shift, θ, were recorded in the frequency domain 0.1–10⁵ Hz. The superimposed ac-signal was 10 mV peak topeakamplitude. To achieve reproducibility, each experiment was carried out at least twice. The surface morphology and the constituent elements of the different electrodes were investigated by SEM/EDAX (model ISPECT S 2006, FEI Company, Holland). Details of experimental procedures areas described elsewhere [22]-[24].

III. RESULTS AND DISCUSSION

3.1. Potentiodynamic polarization measurements

3.1.1 Effect of chloride ion concentration

Linear polarization experiments and Tafel extrapolation measurements were used to investigate the electrochemical behavior of the Mg-7Al-1Zn alloy in chloride free and chloride containing neutral solutions. The potentiodynamic polarization curves of the alloy after holding the electrode at the open-circuit potential for 90 min in stagnant naturally aerated solutions are presented in Fig.-1. The corrosion parameterizes. Corrosion potential, E_{corr} , corrosion current density, i_{corr} , and the Tafel slopes, β_a and β_c were calculated and presented in Table 1. Fig. 1 shows an active dissolution of the alloy with increasing potential in the anodic side. The cathodic reaction is affected by chloride ions more than the anodic one at low concentration, ($[Cl^-] \leq 0.2$ M). At higher chloride ion concentration the rates of both cathodic and anodic reactions were accelerated. The intersecting point of the anodic and cathodic curve, E_{corr} , is that they did not show a significant shift with the increase of chloride ion concentration. Table 1 show that the corrosion current density, i_{corr} , of the alloy increases with increasing the chloride ion concentration. The

increase in corrosion rate with increasing chloride ions concentration can be attributed to the participation of chloride ions in the dissolution reaction. Chloride ions are aggressive for both magnesium and aluminum.

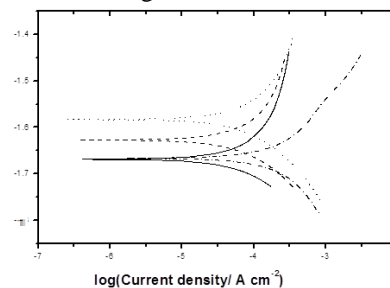
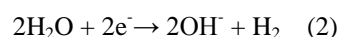
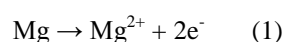


Fig.- 1: Potentiodynamic polarization curves of the Mg-Al-Zn alloy after immersion in stagnant naturally aerated neutral solution free (—) and containing 0.1 M (---), 0.2 M (...) and 0.4 M (-.-.-) NaCl at 25°C and a scan rate of 10 mV s⁻¹.

Table 1. The corrosion parameter of Mg-7Al-1Zn alloy in neutral solution containing different concentration of chlorides.

Cl ⁻ / M	E_{corr} / mV	i_{corr} / $\mu A cm^{-2}$	B_a / mV	B_c / mV
0.0	-1666	44	149	-71
0.1	-1624	65	194	-130
0.2	-1587	74	203	-140
0.3	-1640	78	156	-117
0.4	-1668	151	132	-136

The adsorption of chloride ions on oxide covered magnesium surface transforms Mg (OH)₂ easily to soluble MgCl₂[11]. In agreement with the above observations, most of the polarization curves exhibited an increase in anodic current density with the increase in chloride ion concentration. The cathodic curves are also shifted to higher current density values with the increase in chloride ion concentration. The shift of E_{corr} to more negative values with the increase in chloride ion concentration (cf. Table 1) is explained by the adsorption of these ions on the alloy surface at the weak points in the oxide film [24]. When magnesium is exposed to the aqueous solutions, a grey layer, mainly magnesium hydroxide, forms on its surface, which is stable in basic solutions [24]. Nevertheless, in presence of chloride anions, this surface film breaks down and magnesium appears unprotected. Although corrosion mechanism of magnesium needs further investigation, it is generally reported that the following anodic (1) and cathodic (2) reactions take place:



Firstly, magnesium dissolves and Mg²⁺(aq) cations are produced possibly through intermediate steps involving monovalent magnesium ion [25]-[27]. Secondly, magnesium dissolution is accompanied by hydrogen

evolution, since magnesium in acidic and neutral solutions is well below the region of water stability. Finally, pH rises along with the cathodic reaction due to the formation of OH⁻, which favors the formation of Mg(OH)₂(s) according to Pourbaix diagram [28]. Thus, the overall reaction could be expressed as $Mg^{2+} + 2OH^{-} \rightarrow Mg(OH)_2$ (3)

3.1.2 Effect of inhibitor concentration

Polarization experiments were undertaken specifically to separate the different effects of N-acetylcysteine on the anodic and cathodic partial reactions of the corrosion process. Fig.- 2a presents the potentiodynamic polarization curves of Mg-Al-Zn alloy in 0.2 M NaCl free and containing N-acetyl-cysteine. The corrosion parameters in the different solutions are calculated and presented in Table 2. It is clear from the potentiodynamic data that the presence of the N-acetyl-cysteine decreases the corrosion rate. This is also reflected on the decrease of the values of both β_a and β_c (cf. Table 2), which means that N-acetyl-cysteine is affecting the rates of both the cathodic and anodic reactions. The general shift of the open-circuit potential in the positive direction and the remarkable decrease of β_a values, indicate that N-acetyl-cysteine is functioning as anodic inhibitor more than a cathodic one [25].

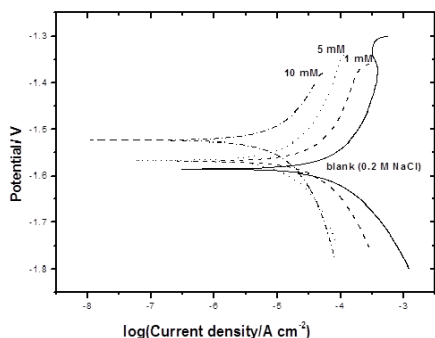


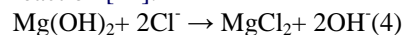
Fig.- 2a: Potentiodynamic polarization curves of the Mg-Al-Zn alloy after immersion in stagnant naturally aerated neutral 0.2 M NaCl solution free (—) and containing 1mM (- - -), 5mM (....) and 10 mM (-.-.-) of N-acetylcysteine at 25°C and a scan rate of 10 mV s⁻¹.

Tables 2: The corrosion parameters of the Mg-7Al-1Zn alloy in stagnant naturally aerated neutral 0.2 M NaCl solution free and containing different concentration of N-acetyl cysteine. The surface coverage and surface area are also presented.

Inh. Conc. mM/L	E _{corr} / mV	i _{corr} / μAcm ⁻²	B _a / mV	B _c / mV	η %	θ	Surface area (cm ²)
0	-159	74	203	140	-----	-----	-----
1	-156	11.3	89	-79	84.3	0.84	0.169
3	-156	10.2	82	-63	85.8	0.86	0.172
5	-152	5.7	78	-77	92.1	0.92	0.184
10	-151	3.3	68	-76	95.4	0.95	0.191

The corrosion inhibition efficiency, η, was calculated from the values of the corrosion current density without inhibitor, i_{corr}, and its value in the presence of the inhibitor, i_{corr} (inh), according to:

and the adsorption of chloride ions on the oxide or hydroxide covered magnesium surface transforms Mg(OH)₂ easily to soluble MgCl₂ via the following reaction [11].



$$\eta = \left[\frac{i_{corr} - i_{corr} (inh)}{i_{corr}} \right] 100 \quad (5)$$

Generally, with increasing inhibitor concentration, the corrosion current density and corrosion rate decrease (cf. Table 2) and the inhibition efficiency increases (cf. Fig.2b). The high inhibition efficiency of N-acetyl-cysteine is due to the presence of the SH group. It is well known that organic corrosion inhibitors are adsorbed on metallic surfaces through hetero-atoms like nitrogen, oxygen or sulfur. In neutral solutions, inhibitor molecules can be protonated at the amino group, even though the presence of S-H decreases the stability of the positive charge. The inhibitor could interact with the corroding surface via the protonated amino groups or via the S atom in the aliphatic chain which can be adsorbed at the anodic sites and inhibit Mg electro- dissolution. The sulfur containing amino acids can be adsorbed as bi-dentate ligands in which surface coordination is taking place through both the amino group (or carboxylic group) and the -S- moiety. The compound thus has the ability to influence both the anodic partial reactions, giving rise to the recorded anodic inhibition mechanism. The inhibition efficiency follows the sequence O < N < S < P [29]. The presence of the -SH group in the molecular structure of N-acetyl-cysteine provokes an increase of the inhibition efficiency. The SH group is more effective as electron donor and functions as an adsorption center beside the nitrogen atom of the amino group [30]. The corrosion inhibition process is based on the adsorption of the amino acid molecules on the active sites and/or deposition of the corrosion products on the alloy surface [31]. Therefore the adsorbed molecules will retard the alloy corrosion and a decrease in the corrosion rates will be recorded. It is essential to understand and explain the mode of adsorption and the stability of the adsorbed layers.

3.2. Adsorption isotherm

The corrosion inhibition process is based on the adsorption of the inhibitor molecules on the metallic surface and two modes of adsorption can be considered. Physical adsorption which requires the presence of electrically charged metal surface and charged species in the bulk of the solution, and chemisorptions which requires charge sharing (chemical bond formation) between the inhibitor molecule and the metal surface. In order to specify the adsorption mode of N-acetyl-cysteine, the degree of surface coverage, θ, at different concentrations of the inhibitor in the stagnant naturally aerated neutral chloride solution was determined from the

corresponding electrochemical polarization measurements according to:

$$\theta = [i_{corr} - i_{corr}(inh)] / i_{corr} \quad (6)$$

The obtained values of θ were fitted to different isotherms including Langmuir, Frumkin and Temkin isotherms. The best fitting was found to obey the Langmuir adsorption isotherm, Eq. 7, which is based on the assumption that all adsorption sites are equivalent and that particle binding occurs independently from nearby sites being occupied or not [32]-[34]:

$$KC = \frac{\theta}{1-\theta} \quad (7)$$

Where C is the concentration of inhibitor, θ , the fractional surface coverage and K is the adsorption equilibrium constant related to the free energy of adsorption ΔG_{ads} as [34]:

$$K = \frac{1}{C_{solvent}} \exp\left(-\frac{\Delta G}{RT}\right) \quad (8)$$

Where $C_{solvent}$ represents the molar concentration of the solvent. In the case of water $C_{solvent}$ is 55.5 mol dm^{-3} , R the universal gas constant and T is the absolute temperature. Equation 7 can be rearranged to:

$$\frac{C}{\theta} = \frac{1}{K} + C \quad (9)$$

A plot of C/θ as a function of C gives a straight line with a slope of unity. Such linear relationship was verified for the adsorption of N-acetyl-cysteine on the alloy surface (cf. Fig.-3). The free energy of adsorption, ΔG_{ads} , was calculated and found to be equal to $-31.5 \text{ kJ mol}^{-1}$.

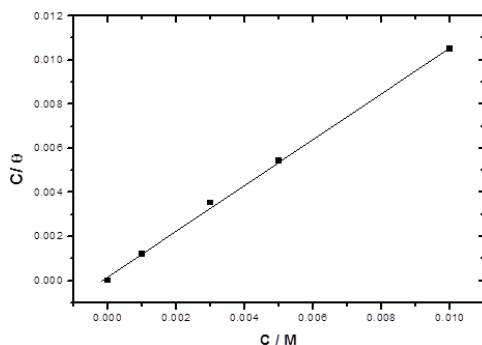


Fig.- 3: Langmuir isotherms of the adsorption N-acetylcysteine on the Mg-Al-Zn alloy in stagnant naturally aerated neutral 0.2 M NaCl solution at 25°C.

A value of -40 kJ mol^{-1} is usually adopted as a threshold value between chemi- and physisorption [33]. Therefore the adsorption of the investigated inhibitor molecules on Mg-Al-Zn alloy is of a physical nature.

3.3. Electrochemical impedance spectroscopic investigations

The results of the potentiodynamic polarization experiments were confirmed by impedance

measurements, since the electrochemical impedance spectroscopy, EIS, is a powerful technique in studying corrosion mechanisms and adsorption phenomena [35]. The experimental impedance results are simulated to pure electronic models that can verify or rule out mechanistic models and enable the calculation of numerical values corresponding to the physical and/or chemical properties of the electrochemical system under investigation [19],[36],[37]. The effect of the chloride ions concentration on the corrosion behavior of the alloy was investigated. Bode and Nyquist plots for Mg-Al-Zn alloy recorded after 90 min of electrode immersion in stagnant naturally aerated neutral solutions containing different concentrations of chloride ions are presented in Fig.-4. Bode plots are recommended as standard impedance plots, since all experimental impedance data are equally represented and the phase angle, as a sensitive parameter to interfacial phenomena, appears explicitly [35]-[37]. Generally, the impedance diagrams show resistive regions at high and low frequencies and capacitive contributions at intermediate frequencies. The low frequency loop is related to the charge transfer resistance and the double-layer capacitance of the electrode, while the high frequency one is attributed to the presence of a protective surface layer of MgO or Mg(OH)₂ (cf. Fig.-4).

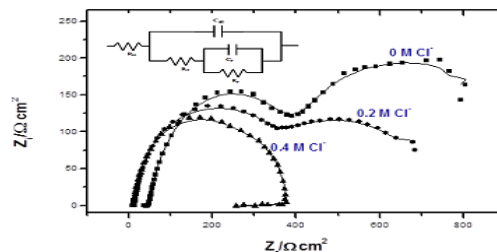


Fig.- 4: Bode plots of Mg-Al-Zn alloy after immersion in stagnant naturally aerated neutral solution free and containing different concentration of NaCl at 25°C. (■) chloride free solution, (●) 0.2 M Cl⁻ and (▲) 0.4 M Cl⁻ containing solutions. (Inset): Equivalent circuit model used for the impedance data fitting; R_{Ω} = solution resistance, R_{ct} = charge-transfer resistance, C_{dl} = double layer capacitance, R_f = film resistance, and C_f = film capacitance.

The impedance data were analyzed using software provided with the electrochemical workstation, where the dispersion formula was used [38]. In this formula an empirical factor α ($0 \leq \alpha \leq 1$) is introduced to account for the deviation from the ideal capacitive behavior due to surface inhomogeneities, roughness factors and adsorption effects [19],[36]. The experimental values are correlated to the equivalent circuit model presented as inset in Fig.-4. In this model, additional equivalent circuit parameters, R_f for the film resistance and C_f for the film capacitance, were introduced to account for the adsorption and deposition phenomena [19]. The calculated equivalent circuit parameters are presented in Table 3. The charge transfer resistance and passive film was found to be dependent on the concentration of the chloride ions (cf. Table 3). The increase in the concentration of Cl⁻

decreases both R_{ct} and R_f . This trend is most likely due to an increase in the adsorbed amount of the Cl^- ions on the electrode surface. In Fig.-4, the impedance of the alloy shows two well-defined capacitive loops at low concentrations (0.1 to 0.3 M NaCl) while at higher concentrations ($[Cl^-] > 0.3$ M) the second loop is depressed, which is attributed to adsorption and desorption phenomena occurring at the electrode surface [39].

Table 3: Equivalent circuit parameters for Mg-Al-Zn alloy after immersion in stagnant naturally aerated neutral containing different NaCl concentration at 25 °C.

[Cl ⁻]/ M	R_s / Ω	R_p / Ω / cm^2	C_{dl} / μF / cm^2	α_1	R_f / Ω / cm^2	C_f / μF / cm^2	α_2
0	67	415	15	0.99	618	813	0.98
0.1	18	426	19	1.0	602	661	0.94
0.2	14	396	16	0.99	543	587	0.96
0.3	12	435	15	0.99	101	1258	0.62
0.4	9	377	13	0.98	---	---	---

Table 3 shows clearly that the corrosion resistance of the Mg alloy decreases as the chloride ion concentration increases which means also that the impedance investigations are in good agreement with the polarization measurement. The effect of inhibitor concentration on the corrosion rate of the Mg-Al-Zn alloy in stagnant naturally aerated neutral solution containing 0.2 M Cl^- ions is presented in Fig.-5. The presence of the inhibitor in the solution leads to the disappearance of the second phase maximum in the Bode plot. A single broadened phase maximum was recorded at intermediate frequency. The increase in N-acetyl-cysteine concentration results in an increase in the impedance of the interface (cf. Fig.-5a). The experimental impedance data were fitted to theoretical data according to the equivalent circuit model presented as inset in Fig.-5a, and the calculated values of the data fitting are presented in Table 4.

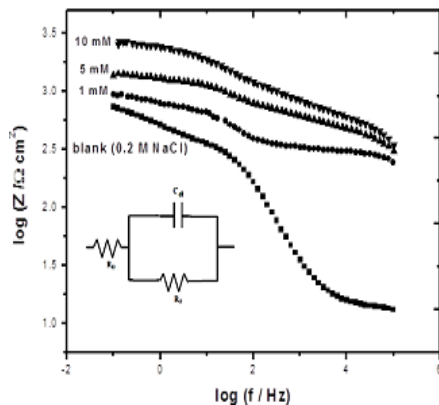


Fig.- 5a: Bode impedance plots of Mg-Al-Zn alloy after immersion in stagnant naturally aerated neutral 0.2 M chloride solution containing different concentration of N-acetyl cysteine at 25°C. The inset is the simple equivalent model for the inhibited surface.

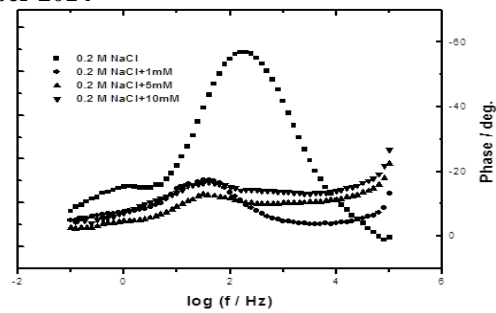


Fig.- 5b: Bode phase plots of Mg-Al-Zn alloy after immersion in stagnant naturally aerated neutral 0.2 M chloride solution containing different concentration of N-acetyl cysteine at 25°C.

Tables 4: The electrochemical impedance parameters of Mg-Al-Zn alloy in buffer of pH 7 and 0.2 M NaCl solution containing different concentration of N-acetyl cysteine.

Inh. conc / mM L ⁻¹	R_s / Ωcm^2	R_{corr} / Ωcm^2	C_{dl} / $\mu F cm^2$
0.0	17.8	396.4	16
1.0	10.3	1198	5.1
3.0	13.6	1345	4.7
5.0	33.8	1423	4.2
10.0	45.3	2213	3.8

The presence of N-acetyl-cysteine in the chloride containing solution leads to an increase in the corrosion resistance, which become more pronounced as the inhibitor concentration is increased. The adsorption of the inhibitor molecules onto the metal/electrolyte interface protects the alloy from the attack of the corroding electrolyte. As mentioned before, N-acetyl-cysteine molecules are adsorbed as bidentate ligands in which surface coordination is taking place through both the amino group and the -SH moiety. In neutral solutions, the inhibitor molecule is present as Zwitter ion and the alloy surface is mostly covered with adsorbed layer of the halide ions [40]-[41]. The inhibitor Zwitter ion will be adsorbed on the active sites, where the Cl^- is already present on the alloy surface and the adsorption of the inhibitor is enhanced in the presence of the halide ions [36]. The synergistic effect between the inhibitor molecules and the chloride ions leads to a stabilized adsorption of the inhibitor on the active sites and hence a decrease in the corrosion rate.

3.4. Scanning electron microscopic investigations

To investigate the surface morphological changes in the presence of chloride ions and the effect of inhibitor molecules on the Mg-Al-Zn surface, scanning electron microscopy was used. The SE micrographs of mechanically polished Mg alloy are presented in Fig.-6.

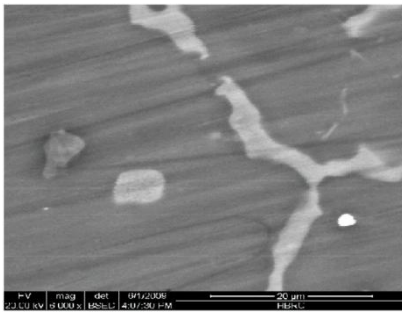


Fig. - 6: SE micrograph of mechanically polished Mg-Al-Zn alloy.

The main characteristic of this image is the presence of the β -phase (lighter region) located mainly around the dendrites of α -matrix[23]. Fig. 7a show the SE micrograph of the alloy surface after 90 min immersion in stagnant naturally aerated neutral 0.2 M chloride solution, where clear corrosion patterns can be identified. There are small cylindrical pits where some areas of magnesium hydroxide called “Brucite” can be identified [25],[42]. Fig. 7b presents the SE micrograph of the sample after immersion in stagnant naturally aerated neutral 0.2 M chloride solution containing 10 mM N-acetyl-cysteine. The micrograph shows an improvement in the surface morphology where the flawed regions were repaired and the cracks were healed.

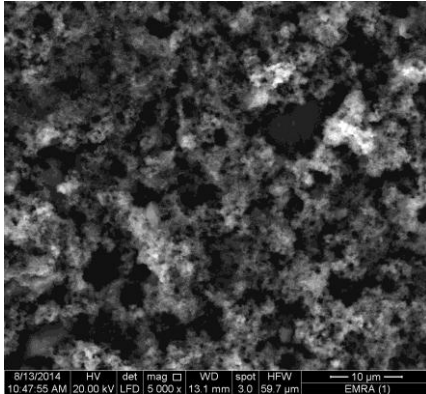


Fig.- 7a: SEM of the Mg-Al-Zn alloy surface after 90 min immersion in stagnant naturally aerated neutral 0.2 M NaCl solution.

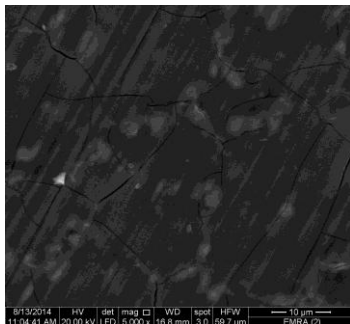


Fig.- 7b: SEM of the Mg-Al-Zn alloy surface after 90 min immersion in stagnant naturally aerated neutral 0.2 M NaCl solution containing 10 mM N-acetylcysteine at 25°C.

Although that the EDAX analysis does not represent exactly the film composition, it shows at least how the chloride ions and also sodium are present on the alloy surface. Figs. 8a and b present the EDAX of the sample after immersion in stagnant naturally aerated neutral 0.2 M chloride solution and that containing 10 mM N-acetyl-cysteine, respectively.

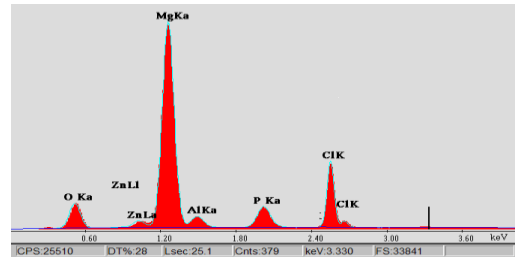


Fig.- 8a: EDAX of the Mg-Al-Zn alloy surface after 90 min immersion in stagnant naturally aerated neutral 0.2 M NaCl solution.

The EDAX analysis of Fig. 8a shows clear presence of the chloride on the alloy surface and it was suppressed after the addition of the inhibitor. It is worthy to mention that about 12wt% of chloride was present on the barrier film and goes down to about 1wt% in the presence of 10 mM N-acetyl-cysteine.

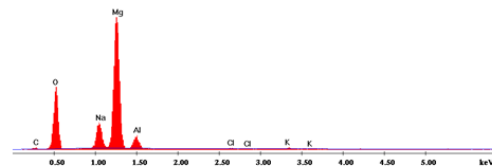


Fig.- 8b: EDAX of the Mg-Al-Zn alloy surface after 90 min immersion in stagnant naturally aerated neutral 0.2 M NaCl solution containing 10 mM N-acetylcysteine at 25°C.

IV. CONCLUSIONS

Environmentally safe N-acetyl-cysteine is promising corrosion inhibitors for Mg–Al–Zn alloys, especially in the presence of the corrosive chloride ions. The corrosion inhibition efficiency increases with increasing the inhibitor concentration. The mechanism of the corrosion inhibition process is based on the adsorption of N-acetyl-cysteine molecules on the active sites of the alloy surface. The calculated free energy of adsorption ($-31.5 \text{ kJ mol}^{-1}$) reveals physical adsorption obeying the Langmuir adsorption isotherm. SEM and EDAX analysis have shown the presence of chloride on the surface which is suppressed in presence of the inhibitor.

REFERENCES

- [1] E. F. Emley, Principle of Magnesium Technology, Pergamon Press, London, UK, 1966.
- [2] G. L. Song and A. Atrens, Corrosion Mechanisms of Magnesium Alloys, Advanced Engineering Materials, vol. 1, pp.11–33,1999.

- [3] G. Song, A. Atrens, D.S.T. Jonh, J. Nairn, Y. Li, The anodic dissolution of magnesium in chloride and sulfate solutions, *Corros. Sci.*, vol. 39, pp. 1981–2004, 1997.
- [4] Ambat, N.N. Aung, W. Zhou, Studies on the influence of chloride ion and pH on the corrosion and electrochemical behavior of AZ91D magnesium alloy, *J. Appl. Electrochem.*, vol. 30, pp. 865–874, 2000.
- [5] M. Anik, G. Celikten, Analysis of the electrochemical reaction behavior of alloy AZ91 by EIS technique in H₃PO₄/KOH buffered K₂SO₄ solutions, *Corros. Sci.*, vol. 49, pp. 1878–1894, 2007.
- [6] J. Chen, J. Dong, J. Wang, E. Han, W. Ke, Effect of magnesium hydride on the corrosion behavior of an AZ91 magnesium alloy in sodium chloride solution, *Corros. Sci.*, vol. 50, pp. 3610–3614, 2008.
- [7] A. Pardo, M.C. Merino, A.E. Coy, R. Arrabal, F. Viejo, E. Matykina, Corrosion behavior of magnesium/aluminum alloys in 3.5 wt.% NaCl, *Corros. Sci.*, vol. 50, pp. 823–834, 2008.
- [8] L.J. Yang, Y.H. Wei, L.F. Hou, D. Zhang, Corrosion behavior of die-cast AZ91D magnesium alloy in aqueous sulphate solutions, *Corros. Sci.*, vol. 52, pp. 345–351, 2010.
- [9] U.C. Nwaogu, C. Blawert, N. Scharnagl, W. Dietzel, K.U. Kainer, Effects of organic acid pickling on the corrosion resistance of magnesium alloy AZ31 sheet, *Corros. Sci.*, vol. 52, pp. 2143–2154, 2010.
- [10] X. Hallopeau, T. Beldjoudi, C. Fiaud, L. Robbiola, corrosion resistance and electrochemical behavior of Mg and AZ91D alloy in aqueous electrolyte solutions containing XOyn- inhibiting ions, in special issues: corrosion resistance of Magnesium alloys, *Corros. Rev.*, vol. 16, pp. 27–42, 1998.
- [11] R. Ambat, N.N. Aung, W. Zhou, Evaluation of microstructural effects on corrosion behavior of AZ91D magnesium alloy, *Corros. Sci.*, vol. 42, pp. 1433–1455, 2000.
- [12] K.Z. Chong, T.S. Shih, Conversion-coating treatment for magnesium alloys by a permanganate–phosphate solution, *Mater. Chem. Phys.*, vol. 80, pp. 191–200, 2003.
- [13] D.Q. Zhang, L.X. Gao, G.D. Zhou, Synergistic effect of 2-mercapto benzimidazole and KI on copper corrosion inhibition in aerated sulfuric acid solution, *J. Appl. Electrochem.*, vol. 33, pp. 361–366, 2003.
- [14] E.E. Oguzie, C. Unaegbu, C.N. Ogukwe, B.N. Okolue, A.I. Onuchukwu, Inhibition of mild steel corrosion in sulphuric acid using indigo dye and synergistic halide additives, *Mater. Chem. Phys.*, vol. 84, pp. 363–368, 2004.
- [15] G. Moretti, F. Guidi, G. Grion, Tryptamine as a green iron corrosion inhibitor in 0.5 M deaerated sulphuric acid, *Corros. Sci.*, vol. 46, pp. 387–403, 2004.
- [16] Y. Li, P. Zhao, Q. Liang, B. Hou, Berberine as a natural source inhibitor for mild steel in 1 M H₂SO₄, *Appl. Surf. Sci.*, vol. 252, pp. 1245–1253, 2005.
- [17] S.M.A. Shibli, V.S. Saji, Co-inhibition characteristics of sodium tungstate with potassium iodate on mild steel corrosion, *Corros. Sci.*, vol. 47, pp. 2213–2224, 2005.
- [18] G. Mu, X. Li, Inhibition of cold rolled steel corrosion by Tween-20 in sulfuric acid: Weight loss, electrochemical and AFM approaches, *J. Colloid Interface Sci.*, vol. 289, pp. 184–192, 2005.
- [19] W.A. Badawy, K.M. Ismail, A.M. Fathi, Environmentally safe corrosion inhibition of the Cu–Ni alloys in acidic sulfate solutions, *J. Appl. Electrochem.*, vol. 35, pp. 879–888, 2005.
- [20] E.E. Oguzie, Studies on the inhibitive effect of *Occimumviridis* extract on the acid corrosion of mild steel, *Mater. Chem. Phys.*, vol. 99, pp. 441–446, 2006.
- [21] W.A. Badawy, K.M. Ismail, A.M. Fathi, Corrosion control of Cu–Ni alloys in neutral chloride solutions by amino acids, *Electrochim. Acta*, vol. 51, pp. 4182–4189, 2006.
- [22] W.A. Badawy, F.M. Al-Kharafi, A.S. El-Azab, Electrochemical behavior and corrosion inhibition of Al, Al-6061 and Al-Cu in neutral aqueous solutions. *Corros. Sci.*, vol. 41, pp. 709–727, 1999.
- [23] W.A. Badawy, N.H. Helal, M.M. El-Rabiee, H. Nady, Electrochemical behavior of Mg and some Mg alloys in aqueous solutions of different pH, *Electrochim. Acta*, vol. 55, pp. 1880–1887, 2010.
- [24] Gh.M. Abd El-Hafez, N.H. Helal, M.M. El-Rabiee, W.A. Badawy, Effect of Al content on the corrosion behavior of Mg–Al alloys in aqueous solutions of different pH, *Electrochim. Acta*, vol. 55, pp. 6651–6658, 2010.
- [25] B.A. Shaw (2003). Corrosion Resistance of Magnesium Alloys, in: *ASM Handbook. Corrosion Fundamentals, Testing Protect.* (13): A, 692.
- [26] G. L. Makarand J. Kruger, Corrosion Studies of Rapidly Solidified Magnesium Alloys. *J. Electrochem. Soc.*, vol. 137, pp. 414–421, 1990.
- [27] G. R. Hoey and M. Cohen, Corrosion of Anodically and Cathodically Polarized Magnesium in Aqueous Media, *Electrochem. Soc.*, vol. 105, pp. 245–250, 1958.
- [28] Van Muylder J, Pourbaix M, Magnesium in: M. Pourbaix (Ed.), *Atlas of Electrochemical Equilibrium in Aqueous Solution*, Pergamon Press, Oxford, pp. 139–145, 1996.
- [29] E. McCafferty, *Corrosion Control by Coating*, Science Press, Princeton, NJ, pp. 279, 1979.
- [30] B. Hammouti, A. Aouniti, M. Taleb, M. Brighli, and S. Kertit, L-Methionine Methyl Ester Hydrochloride as a Corrosion Inhibitor of Iron in Acid Chloride Solution. *Corrosion*, vol. 51, pp. 411–416, 1995.
- [31] G. Bereket, A. Yurt, The inhibition effect of amino acids and hydroxy carboxylic acids on pitting corrosion of aluminum alloy 7075, *Corros. Sci.*, vol. 43, pp. 1179–1195, 2001.
- [32] A. Popova, M. Christov, S. Raicheva, and E. Sokolova, “Adsorption and inhibitive properties of benzimidazole derivatives in acid mild steel corrosion,” *Corros. Sci.*, vol. 46, pp. 1333–1350, 2004.
- [33] B.B. Damaskin, O.A. Pertii, V.V. Batrakov, *Adsorption of Organic Compounds on Electrodes*, Plenum Press, New York, 1971.
- [34] J. Lipkowski, P.N. Ross (Eds.), *Adsorption of Molecules at Metal Electrodes*. VCH, New York, 1992.

- [35] J.R. Macdonald, Impedance Spectroscopy, John Wiley & Sons, New York, 1987.
- [36] W.A. Badawy, K.M. Ismail, A.M. Fathi, Effect of Ni content on the corrosion behavior of Cu–Ni alloys in neutral chloride solutions, *Electrochim. Acta*, vol. 50, pp.3603-3608, 2005.
- [37] W.A. Badawy, F.M. Al-Kharafi, A.S. El-Azab, Electrochemical behavior and corrosion inhibition of Al, Al-6061 and Al–Cu in neutral aqueous solutions, *Corros. Sci.*, vol. 41, pp.709-727, 1999.
- [38] M.M. El-Rabee, N.H. Helal, Gh.M. Abd El-Hafez, W.A. Badawy, Corrosion control of vanadium in aqueous solutions by amino acids, *J. Alloys Compd.*, vol. 459, pp.466-471, 2008.
- [39] J. H. Greenblatt, A Mechanism for the Anodic Dissolution of Magnesium. *Electrochem. Soc.*, vol. 103, pp.539-543, 1956.
- [40] Ghada M. Abd El-Hafez, Waheed A. Badawy, The use of cysteine, N-acetyl cysteine and methionine as environmentally friendly corrosion inhibitors for Cu–10Al–5Ni alloy in neutral chloride solutions, *Electrochim. Acta*, vol. 108, pp. 860-866, 2013.
- [41] A.I. Munoz, J.G. Anton, J.L. Guinon, V.P. Herranz, Comparison of inorganic inhibitors of copper, nickel and copper–nickels in aqueous lithium bromide solution, *Electrochim. Acta*, vol. 50, pp.957-966, 2004.
- [42] O. Lunder, T.K. Aune, K. Nisancioglu, Effect of Mn Additions on the Corrosion Behavior of Mould-Cast Magnesium ASTM AZ91, *Corrosion*, vol. 43, pp. 291-295, 1987.